Mechanical, electrochemical and magnetic behaviour of duplex stainless steel for biomedical applications

R. W. Gregorutti*[1], J. Enrique Grau[1], F. Sives[2] and C. I. Elsnerc[3,4]

Mechanical, electrochemical and magnetic properties of duplex stainless steel were analysed to evaluate its use as biomaterial, comparing the results with those obtained for austenitic stainless steel. Yield and ultimate tensile strengths are almost twice in duplex stainless steel, being the values 870 MPa and 564 MPa, respectively. The electrochemical test revealed that this material has lower susceptibility to localised corrosion because of its greater passive range, 1 V from the open circuit potential, while the austenitic stainless steel exhibited a passive region of 0.370 V. Both steels behave as soft magnetic materials, however, duplex stainless steel has higher magnetic saturation and remanence, while austenitic stainless steel is more prone to heating when exposed to a magnetic field.

Keywords: Biomaterials, Duplex stainless steel, Mechanical, Electrochemical and magnetic properties

Introduction

Austenitic stainless steels ASTM F138/139 and ASTM F745 are widely used for manufacturing load bearing components as knee and hip joints prostheses, bone plates and nails for shinbone. ASTM F138/139 are used for device manufacturing by forging and machining processes, while ASTM F745 (F745-SS) is used for cast implants. These materials have an acceptable biocompatibility, with adequate mechanical, physical and electrochemical properties, in addition to the low cost. However, the austenitic stainless steels have lower corrosion resistance than other metallic materials used in implants as Co–Cr–Mo and Ti alloys when exposed to body fuilds.[1–3] Thus, the exposure for a long time to that aggressive media, which contain mainly chloride ions, may increase the susceptibility to suffer localised corrosion. In view of considering new alternatives of high performance stainless steels for use as biomaterial, duplex stainless steels (D-SS) should be a possible alternative because of their high stress corrosion cracking, corrosion fatigue and pitting resistances in chloride media,[4–7] in addition to its high mechanical strength, properties that are of great importance for materials to be used for implants elaboration. The eventual corrosion, in addition to causing the chemical and mechanical degradation of the implant, promotes the release of metallic ions to the tissues, which, as the case of Ni, can cause metal allergy, carcinogenicity, cytotoxicity and genotoxicity, when releases are in concentrations higher than those admissible.[8–14]

Several articles deal with the use of D-SS in orthopaedic and orthodontic applications, including *in vitro* and *in vivo* studies,[15–21] but as was mentioned in the specific bibliography, its use in the biomedical field must still be accepted.[22]

With the aim of evaluating the potential use of cast D-SS as a biomaterial, the present paper evaluates its mechanical properties and its electrochemical performance in simulated human body conditions and emphasises its magnetic behaviour. The knowledge of magnetic properties of biomaterials is also important because exposure to eventual static and/or variable magnetic fields could cause heat or movement that can be injurious for the human body. The obtained results are compared with those of F745-SS.

Experimental

Both stainless steels were obtained by means of investment casting process (IC), which is one of the techniques used to manufacture surgical implants,[23] in order to perform the analysis with similar microstructures of cast prosthesis. Melting was carried out in a medium frequency induction furnace. The casting temperature was 1600°C, and following the usual practice of the IC process, the shell mould was heated up to 800°C to increase its permeability and reduce the thermal gradient of cooling, in order to improve castability. The resulting chemical compositions are recorded in Table 1.

The 'as cast' microstructures were characterised by means of optical and SEM microscopy with energy dispersive spectroscopy (EDS) analysis and X-ray

[1]Laboratorio de Entrenamiento Multidisciplinario para la Investigación Tecnológica (LEMIT-CICPBA), Av. 52 s/n e/121 y 122, B1900AYB, La Plata, Argentina
[2]Instituto de Física La Plata, CONICET, Dto. de Física, Facultad de Ciencias Exactas, UNLP, 49 y 115, B1900AYB, La Plata, Argentina
[3]Centro de Investigación y Desarrollo en Tecnología de Pinturas (CIDEPINT-CICPBA-CONICET), Av. 52 s/n e/121 y 122, B1900AYB, La Plata, Argentina
[4]Facultad de Ingeniería - UNLP, Av. 1 esq. 47, B1900AYB, La Plata, Argentina

*Corresponding author, email metalurgia@lemit.gov.ar

Published by Maney on behalf of the Institute
Received 11 April 2013; accepted 1 August 2013
DOI 10.1179/1743284715Y.0000000017

Table 1 Chemical composition of analysed material

	C	Cr	Ni	Mo	Si	Mn	N
F745-SS	0.04	18.09	12.46	2.02	0.49	0.90	...
D-SS	0.03	25.22	7.07	4.10	1.00	0.78	0.30

diffraction technique. X-ray diffraction was performed using a 3050 Philips goniometer and Cu K_α radiation. The divergent slit was 1°, and the scanning conditions were steps of 0.02° with a counting time of 1 s/step, 2θ being between 30 and 100°. Both materials were submitted to solution annealing heat treatment to dissolve phases precipitated during solidification. The thermal cycling were as follows:[24] F745-SS was heated at 1080°C during 2 h and then water quenched, while D-SS was heated at 1120°C for 1 h, then cooled in furnace down to 1045°C and maintained for 1 h and subsequently water quenched. Mechanical properties were evaluated through tensile tests on samples of 6.25 mm of diameter according to Standard ASTM E8, using an Instron machine of 15 ton capacity. Hardness was determined following the Vickers method, with a load of 30 kg. The susceptibility to localised corrosion was evaluated through cyclic polarisation tests, following Standard ASTM F2129. Tests were performed using an EG&G potentiostat/galvanostat model 273A. The corrosion cell was assembled with the test material as the working electrode, a saturated calomel electrode (SCE) as reference and a Pt electrode as auxiliary. The tests were performed using aqueous solution 0.9 wt-%NaCl at 37°C and pH between 7.1 and 7.4. The solution was deaired by bubbling N_2 during the tests. The samples were kept in a stabilisation period of 1 h at open circuit condition. After this, the potential scan was performed at 0.167 mV s^{-1} in the anodic direction, from a potential value of 0.2 V more cathodic than open circuit condition up to the anodic limit determined by the following reversal conditions: potential of 3 V(SCE) or current density of 10^{-4} A cm^{-2}.

Magnetic hysteresis curves were obtained at room temperature by a Lake Shore 7404 magnetometer, with magnetic fields between −1 and 1 T.

Results and discussion

Microstructural analysis

The phases present in the stainless steels depend on the balance among ferrite stabilising alloys as Cr, Mo and Si and austenite stabilising alloys as C, Ni, Mn and N. In the case of the F745-SS, the structure is fully austenitic, as a consequence of the Ni content between 12 and 14%. The 'as cast' microstructure of this material, shown in Fig. 1*a*, consists of austenite dendrites formed as a consequence of the thermal and constitutional undercoolings produced during solidification, which destabilise the solid/liquid interface. Another typical feature in the solidification processes is the microsegregation of the different alloying elements, based on their respective partition coefficient k. In stainless steels, Cr and Mo segregate directly towards the liquid ($k<1$), increasing their concentration in the interdendritic regions. In contrast, Ni segregates inversely ($k>1$), increasing its concentration in the bulk of the austenite dendrites. The microsegregation of those elements was measured by EDS analysis, and the results are recorded in Table 2.

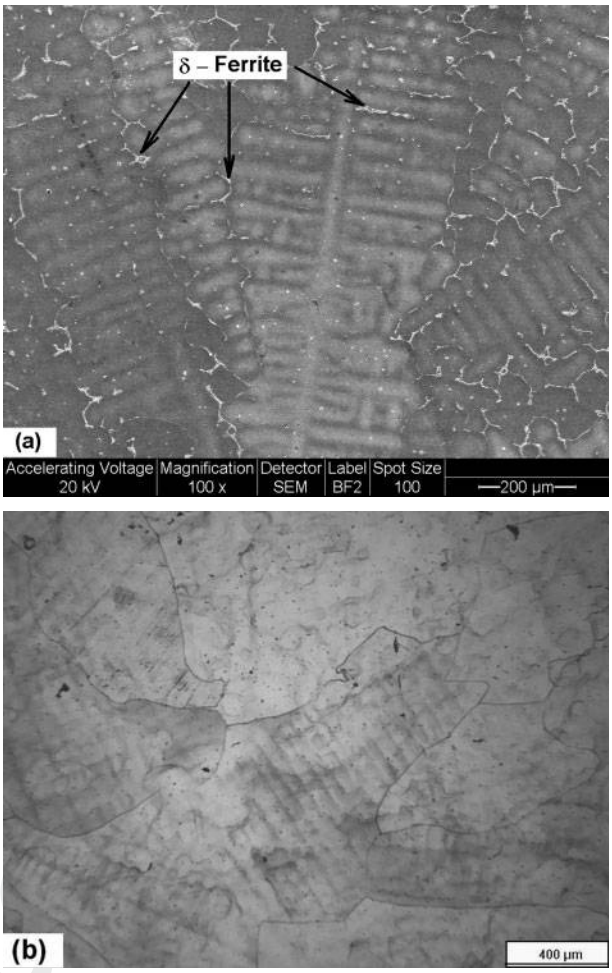

a in 'as cast' condition; *b* after solution annealing heat treatment

1 Microstructure of F745-SS

The high concentration of Cr and Mo in the interdendritic regions promotes the formation of δ-ferrite in these areas, as observed in the microstructure of Fig. 1*a*. The δ-ferrite should be dissolved by means of the solution annealing heat treatment, since it may be detrimental to the corrosion resistance. The obtained structure is shown in Fig. 1*b*, which also reveals the solidification cells of the material.

The microstructure of D-SS is composed by ferrite and austenite in ≅50%. The dual phase corresponds to the higher amounts of Cr, Mo and Si and the lower Ni content with respect to the F745-SS, as reported in Table 1. Figure 2*a* shows the 'as cast' microstructure, where the formation of the sigma phase at the ferrite/austenite interface is also revealed. Sigma phase usually precipitates in the range between 830 and 470°C during

Table 2 Energy dispersive spectroscopy analysis in 'as cast' samples (values in wt-%)

	F745-SS		D-SS		
Element	Interdendritic region	Austenitic dendrite	Ferrite	Austenite	Sigma phase
Cr	22.5	16.7	26.0	25.2	27.5
Mo	4.0	1.2	7.0	5.1	5.6
Ni	9.7	11.4	4.6	6.7	4.1

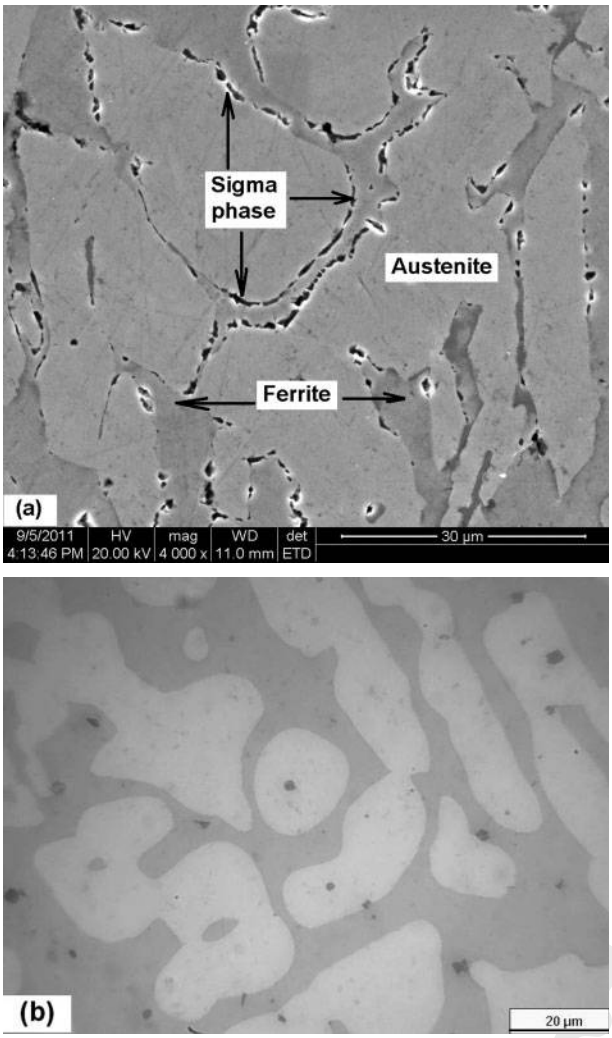

a in 'as cast' condition; *b* after solution annealing heat treatment

2 Microstructure of D-SS

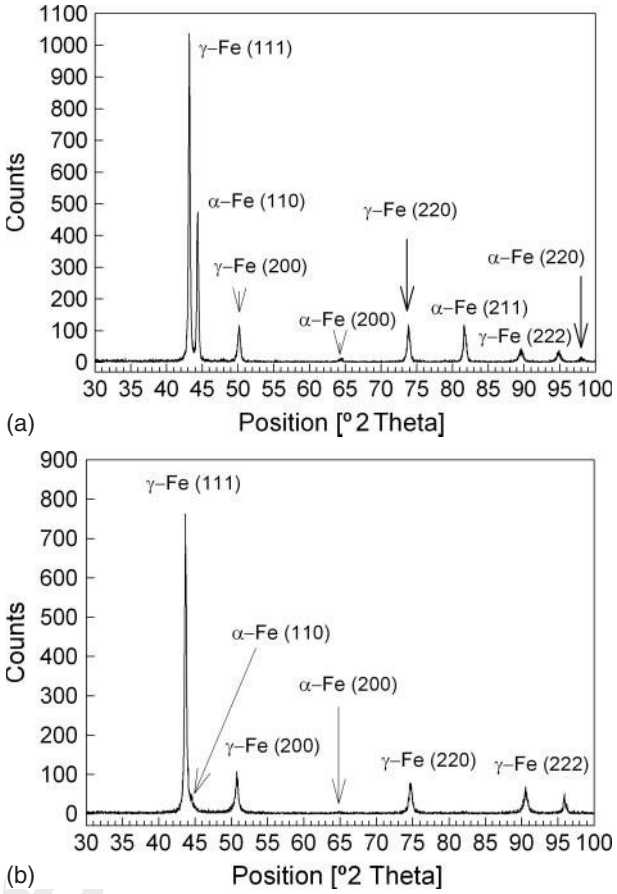

3 X-ray diffractograms corresponding to 'as cast' samples *a* D-SS; *b* F745-SS

cooling after solidification in high Cr stainless steels,[25] and the driving force can be referred to the micro-segregation of Cr at those interfaces. Table 2 illustrates the balance of alloying elements in each phases, where a higher concentration of Cr and Mo in the ferrite and sigma phases while a higher level of Ni in the austenite may be noticed because of the different segregation mechanisms mentioned above.

In previous studies, it has been reported that the sigma phase comes from the eutectoid reaction ferrite→sigma + austenite, the tendency being higher in D-SS.[7,26]

This phase has a harmful effect, since it promotes embrittlement and reduces the corrosion resistance;[5,24,27] for this reason, it should be dissolved by the solution annealing heat treatment, as shown in Fig. 2*b*.

X-ray diffraction was performed to characterise the phases present in the 'as cast' microstructure of both stainless steels. Figure 3*a* shows the diffractogram corresponding to the D-SS, where (111), (200), (220) and (222) austenite peaks were detected. In the case of the ferrite phase, the peaks (110) and (211) were the most intense, while the intensities of the peaks (200) and (220) were the lowest. This feature could be related to some texture in the microstructure promoted during solidification. No relevant peaks of the sigma phase were detected. A slight evidence can only be observed at 2θ close to 48°, corresponding to the peak (411) and at 55° corresponding to the peak (322). The fact that sigma peaks were not clearly observed could be ascribed to the low amount of this phase in the microstructure. The diffractogram belonging to the F745-SS (Fig. 3*b*) showed only austenite peaks, denoting that, the same as the sigma phase in D-SS, the amount of δ-ferrite in the interdendritic region is not enough to be detected by this technique.

Mechanical properties

Surgical implants are subjected to dynamic loads imposed by the body movements and its own weight.[27–29] The load on an implant can reach peaks of about four times the body weight at the hip and three times the body weight at the knee during walking. Although the static test does not reflect the actual working conditions of the implants, it allows comparing the behaviour of different biomaterials and estimating their performance under the solicitation of dynamic loads.

Ultimate tensile strength (UTS) and yield strength (YS) of both stainless steels, in solution annealed condition, are illustrated in Fig. 4.

The UTS and YS values for the D-SS were 871 and 564 MPa respectively, and that of the F745-SS were 456 and 224 MPa respectively. The higher mechanical strength of the D-SS is not directly related with balance of the austenite and ferrite properties, since UTS and YS are greater than those of both phases. The enhancement of the

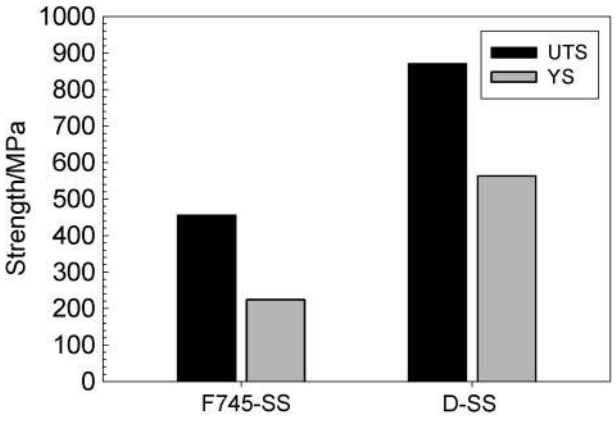

4 *a* ultimate tensile strength and YS of D-SS and F745-SS in solution annealed conditions

mechanical strength can be attributed to the smaller grain size, which usually has D-SS, in addition to the solid solution hardening promoted by the higher substitutional Cr and Mo contents and the interstitial N.[6,30]

Ultimate tensile strength and YS are directly related to the fatigue strength;[6,31] thus, the higher values of these parameters obtained for D-SS lead to infer that this material has greater fatigue resistance than F745-SS and, consequently, lower risk to suffer mechanical failure.

On the other hand, the elongations of both stainless steels were 21% for D-SS and 32% for F745-SS. The higher elongation in F745-SS is a consequence of the fully austenitic structure, which confers higher ductility. In the case of D-SS, the presence of ferrite in the microstructure reduces its ductility although it increases the mechanical strength.

In accordance with the mechanical strength, hardness of D-SS is also higher than that of F745-SS because, as mentioned above, the alloying elements promote the solid solution hardening. The values reported by the hardness test were 282.5 HV30 for the D-SS and 198.3 HV30 for the F745-SS.

Susceptibility to localised corrosion

The resistance to localised or pitting corrosion is one of the most important properties to be satisfied by biomaterials, since the presence of pits in the material can nucleate fatigue cracks and stress corrosion cracks,[11,32] which might lead to the premature failure of the implant. The susceptibility to localised corrosion was evaluated by means of cyclic polarisation tests. This technique allows evaluating the corrosion potential E_{Corr}, the breakdown potential E_{Pit} and the repassivation potential E_b. The E_{Corr} is the potential at the open circuit condition when there is no net current flow, E_{Pit} is the polarisation level at which the anodic current increases considerably with the applied potential and E_b is the potential at which the hysteresis loop is completed upon reverse polarisation scan. These parameters are related to the material's susceptibility to suffer localised corrosion and the capacity to its development respectively. The greater the difference ($E_{Pit}-E_{Corr}$), the more passive the material and, consequently, less prone to suffer localised corrosion, while the lesser the difference ($E_{Pit}-E_b$), the higher the tendency to repassivate the material.

To evaluate the electrochemical performance of the 'as cast' and annealed microstructures of D-SS, cyclic polarisation curves in simulated fluid body were performed. The obtained results are shown in Fig. 5, where it is observed that the behaviour of the material was similar for both conditions. Nevertheless, the anodic polarisation scan of the 'as cast' sample showed current fluctuation in the passive potential range. This instability should be related with the sigma phase precipitated at the ferrite/austenite interface. The adverse effect of this phase on the corrosion properties was studied in high temperature aged D-SS,[7,33,34] in which it is being postulated that the origin of the pitting attack is because the Cr and Mo depletion caused at the surrounding areas of the sigma precipitated.

Taking into account the best performance of the annealed D-SS, its behaviour was compared with the corresponding F745-SS in equivalent conditions. The resulting polarisation curves shown in Fig. 6 reveal that the E_{Corr} value for both materials was in the order of -0.180 ± 0.005 V(SCE). The greatest behaviour difference between both materials was noted along the anodic sweep, in which D-SS maintained a passive response along $\sim$1 V from the open circuit potential, reaching the E_{Pit} potential at 0.94 V(SCE), close to the corresponding oxygen evolution reaction.[17] As it is almost impossible for the open circuit potential of an implant in a biological environment to reach such

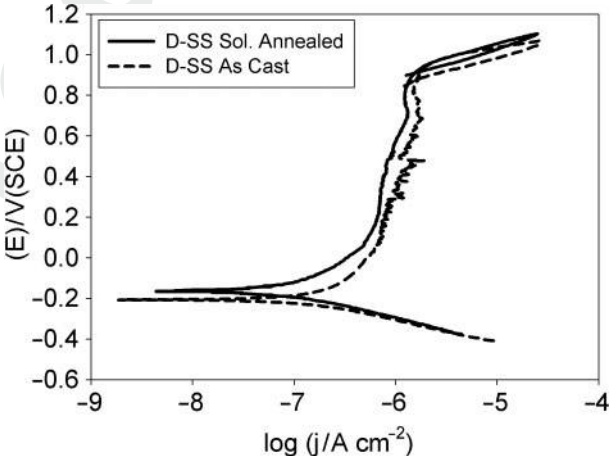

5 Cyclic polarisation curves of D-SS in 'as cast' and solution annealed conditions

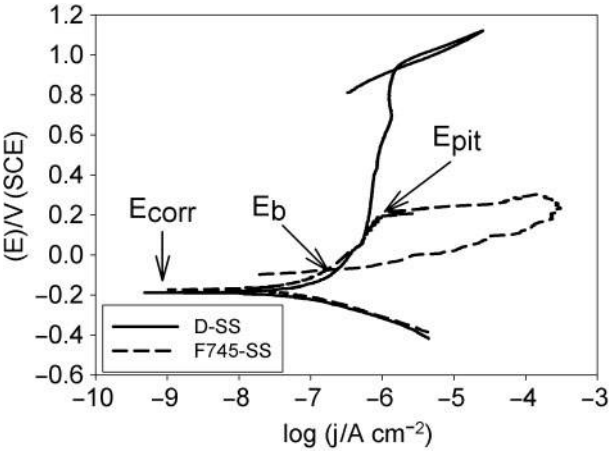

6 Cyclic polarisation curves of D-SS and F745-SS in solution annealed conditions

condition, it is possible to infer that the tendency to pitting initiation is very low, while F745-SS not only has a short passive region (≅0.370 V) but also has less tendency to repassivate [$E_{Pit} = 0.196$ V(SCE) and $E_b = -0.070$ V(SCE)]. From these results, it can be concluded that the performance of D-SS in biological environments will be better than that of F745-SS. Comparing the obtained results with that of other materials that have been used in the medical field in media with similar chloride concentration, it was observed that D-SS has a wider passive region than 316LVM and nickel free high nitrogen austenitic stainless steels alloyed with Mn, for which that region last for ≅0.700 and ≅0.850 V, respectively.[17,35–37] At the same time, the behaviour of D-SS was quite similar with respect to the 316LN, although with slightly lower repassivation capacity.[17]

Pitting corrosion in stainless steels depends mainly on the Cr–Mo–N content, their influence being empirically quantified by the pitting resistance equivalent number (PREN), defined as follows[38]

$$PREN = \mathrm{Cr\%} + 3.3\mathrm{Mo\%} + 16\mathrm{N\%} \quad (1)$$

Higher PREN values are associated to the lower tendency to suffer pitting corrosion.

In accordance with the Cr, Mo and N content of both materials, reported in Table 1, the PREN for the D-SS was considerably higher than that for the F745-SS, the values being and 24.8 respectively.

Nilsson,[6] in his studies on D-SS and different austenitic steel grades, determined the linear relation between PREN and the critical pitting temperature, pointing out that localised corrosion is mainly depending on the chemical composition and not on the ferrite/austenite ratio. Other authors,[33,39,40] using microelectrochemical and cyclic thermometry methods, in higher concentrated NaCl solutions and different test conditions than that used in the present work, have analysed the pitting corrosion in single ferrite and austenite phases in super duplex stainless steels, emphasising that pitting occurs in the phase with lower PREN, this parameter being established by the elements partitioning. In order to elucidate which of the phases is more prone to pitting corrosion, in the case of the D-SS analysed in the present work, the PREN was calculated for austenite and ferrite from the concentrations obtained by EDS. Considering the work of Palmer *et al.*,[41] it was assumed that N partitioned fully to the austenite, for calculations. The results are reported in Table 3.

Despite the similar values of Cr and the preceding consideration about N, the PREN value of austenite was slightly lower than that of ferrite. This evidence can be attributed to the greater influence of Mo, which partitioned more strongly than Cr to the ferrite. These results allow predicting that, in this case, the austenite is more prone to suffer pitting attack than ferrite.

Table 3 Pitting resistance equivalent number of austenite and ferrite in solution annealed D-SS (elements concentration in wt-%)

Element	Austenite	Ferrite
Cr	25.2	26.6
Mo	4.5	6.7
N	0.3	...
PREN	44.9	48.6

Magnetic properties

Another feature that should be considered in biomaterials is the magnetism, since the exposure of the medical devices to magnetic fields, as in the case of analysis by magnetic resonance imaging (MRI), could generate diverse problems. The field strengths of MRI scanners are between 0.2 and 7.0 T, although most of them operate at 1.5 T. The main inconveniences that can occur in this environment are magnetically induced displacement forces and torque, heating and image artefact.[42–44]

Magnetic properties were analysed by means of hysteresis curves that show the evolution of the magnetisation per unit mass M as a function of the magnetic field strength H.

The curves illustrated in Fig. 7, corresponding to both stainless steels, presented a small hysteresis area with low values of remanence and coercivity, behaviours that are similar to the soft magnetic materials, that is, materials that are easy to magnetise and demagnetise. The greatest difference was observed in the magnetisation. The D-SS has a significantly higher M because of the ferrite present in the microstructure, which is a strongly ferromagnetic phase. For a magnetic field of 1 T, M recorded values close to the saturation, being 4.55×10^{-5} T m^3 kg^{-1} for the 'as cast' sample and 5.44×10^{-5} T m^3 kg^{-1} for the solution annealed one. The lower M in the 'as cast' sample can be related to the presence of the sigma phase in the microstructure, which has a non-magnetic behaviour.[25] The dissolution of this phase by the solution annealing treatment would increase the proportion of ferrite in microstructure, increasing M. In the case of the

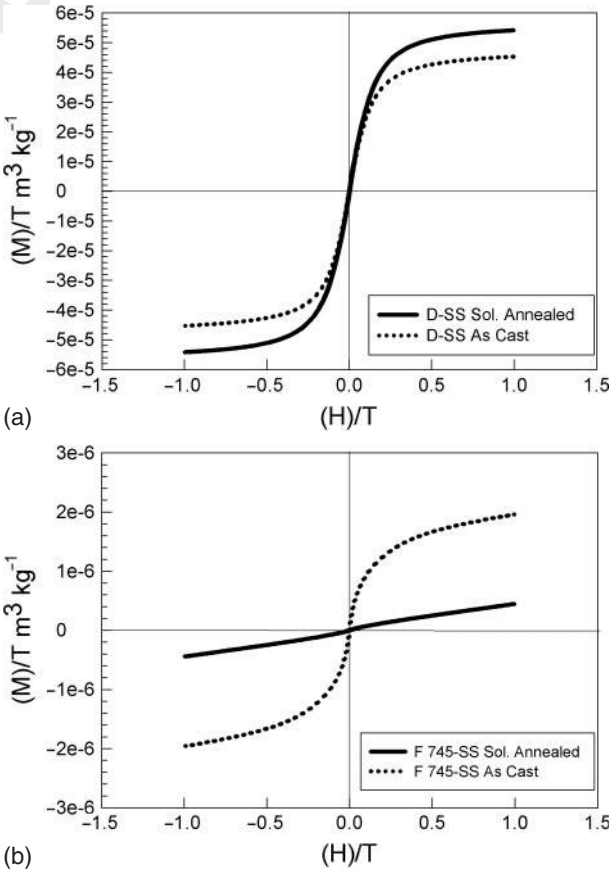

a **D-SS;** ***b*** **F745-SS**

7 Hysteresis curves

F745-SS, magnetisation was an order of magnitude smaller, as a consequence of the fully austenitic structure. At the same time, it was also noted that, in this stainless steel, saturation was not reached for the imposed test conditions. The values of M at 1 T were 1.94×10^{-6} and 4.52×10^{-7} T m^3 kg^{-1} for the 'as cast' and the solution annealed samples respectively. The higher M of the 'as cast' sample can be ascribed to the δ-ferrite precipitating in the interdendritic regions during solidification, as shown in Fig. 1*a*.

As mentioned above, the force induced by a magnetic field is a function of the magnitude of the magnetic field gradient B and the magnetic moment or magnetisation M, as follows[45]

$$F \propto \nabla(MB) \tag{2}$$

The results of Fig. 7 indicate that M recorded values an order of magnitude higher in D-SS. Therefore, according to equation (2), the force induced in this material is greater with respect to the F745-SS, increasing the risk of displacement of the medical device before the eventual exposure to magnetic fields.

Figure 8 shows the magnified image of the curves, in order to perform a qualitative analysis of the remanence and the coercivity of both stainless steels. Remanence B_r indicates the residual magnetisation of the material and is defined by the point where the hysteresis loop intersects the M axis. On the other hand, the coercive force H_c is the intensity of the applied magnetic field required to reduce the magnetisation to zero, after the magnetisation of the sample has been driven to saturation. This parameter is related to the heating promoted by the magnetic field. Although the values of both parameters are small, B_r for D-SS is considerably higher than that for F745-SS, which implicates that this material has a higher residual magnetisation. On the other hand, H_c is greater for F745-SS, indicating that this material is more prone to heating when exposed to a magnetic field.

Conclusions

From the mechanical and electrochemical points of view, cast D-SS has a superior performance as biomaterial than F745-SS because of its higher UTS and YS strength and, mainly, the lower susceptibility to suffer localised corrosion in body simulated media. Comparing the present results with those of other stainless steels used in the medical field, it was also observed that the electrochemical response of D-SS is better than that of 316LVM and nickel free high nitrogen austenitic stainless steels alloyed with Mn.

The magnetic analysis revealed that both stainless steels have similar behaviour to that of the soft magnetic materials because the area under their hysteresis loop is very small. The most important differences are related to magnetic saturation and remanence, which are higher in D-SS, as a consequence of the ferrite present in the microstructure. However, F745-SS has higher coercive force, which implicates that this material is more prone to heating when exposed to magnetic fields. This steel also had a higher magnetic response in the 'as cast' condition, which implicates that it must be submitted to a solution annealed heat tretment to dissolve the δ-ferrite precipitated during solidification.

These last observations lead to infer that further experiments should be performed on both materials to determine the effects of the eventual exposure to magnetic fields, in order to prevent possible injurious for the human body.

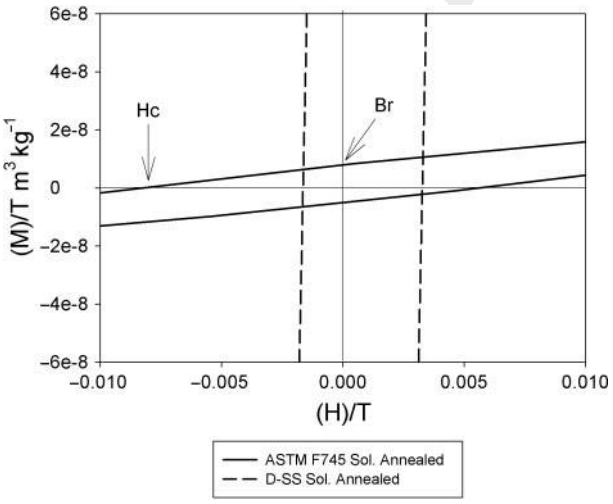

8 Remanence and coercivity of both stainless steels in solution annealed conditions

Acknowledgements

The authors thank the Comisión de Investigaciones Científicas de la Provincia de Buenos Aires (CICPBA), the Consejo Nacional de Investigaciones Científicas y Técnicas (CONICET) and the Universidad Nacional de La Plata of Argentina for the financial support to carry out the present research paper.

References

1. A. C. Fraker: 'Corrosion of metallic implants and prosthetic devices', in 'ASM handbook', (ed. J. R. Davis), 'Corrosion' **Vol. 13**. 9th edn, 1324–1335; 1992, Materials Park, OH, ASM International.
2. I. Gurappa: 'Characterization of different materials for corrosion resistance under simulated body fluid conditions', *Mater. Character.*, 2002, **49**, 73–79.
3. G. Manivasagam, D. Dhinasekaran and A. Rajamanickam: 'Biomedical implants: corrosion and its prevention – a review', *Recent Pat. Corros. Sci.*, 2010, **2**, 40–54.
4. R. M. Davison: 'Corrosion of stainless steels', in 'ASM handbook', (ed. J. R. Davis), 'Corrosion' **Vol. 13**. 9th edn, 1327–1381; 2004, Materials Park, OH, ASM International.
5. G. F. Vander Voort: 'Service characteristics of carbon and low-steels alloy', in 'ASM handbook', (eds. S. R. Lampman and T. B. Zorc), 'Properties and selection: irons, steels and high performance alloys' **Vol. 1**. 10th edn, 1058–1133; 2005, Materials Park, OH, ASM International.
6. J. O. Nilsson: 'Super duplex stainless steel', *Mater. Sci. Technol.*, 1992, **8**, (8), 685–700.
7. J. O. Nilsson and A. Wilson: 'Influence of isothermal phase transformation on toughness and pitting corrosion of super duplex stainless steel SAF2507', *Mater. Sci. Technol.*, 1993, **9**, (7), 545–554.
8. M. Niinomi: 'Recent metallic materials for biomedical applications', *Metall. Mater. Trans. A*, 2002, **33A**, 477–485.
9. M. G. Shettlemore and K. J. Bundy: 'Examination of in vivo influences on bioluminescent microbial assessment of corrosion product toxicity', *Biomaterials*, 2001, **22**, 2215–2228.
10. M. Taira, M. S. Toguchi, Y. Hamada, J. Takahashi, R. Itou, S. Toyosawa, N. Ijyuin and M. Okazaki: 'Studies on cytotoxic effect of nickel ions on three cultured fibroblast', *J. Mater. Sci.: Mater. Med.*, 2001, **12**, 373–376.

11. M. Sumita, T. Hanawa and S. H. Teo: 'Development of nitrogen-containing nickel-free austenitic stainless steels for metallic biomaterials – review', *Mater. Sci. Eng. C*, 2004, **C24**, 753–760.
12. A. Sargeant and T. Goswami: 'Hip implants – paper VI – ion concentrations', *Mater. Des.*, 2007, **28**, 155–171.
13. X. Lü, X. Bao, Y. Huang, Y. Qu, H. Lu and Z. Lu: 'Mechanisms of cytotoxicity of nickel ions based on gene expression profiles', *Biomaterials*, 2009, **30**, 141–148.
14. K. Yang and Y. Ren: 'Nickel-free austenitic stainless steels for medical applications', *Sci. Technol. Adv. Mater.*, 2010, **11**, 1–13.
15. A. Cigada, G. Rondelli, B. Vicentini, M. Giacomazzi and A. Roos: 'Dúplex stainless steel for osteosynthesis devices', *J. Biomed. Mater. Res.*, 1989, **23**, 1087–1095.
16. A. Cigada, G. De Santis, M. A. Gatti, A. Roos and D. Zaffe: 'In vivo behavior of a high performance dúplex stainless steel', *J. Appl. Biomater.*, 1993, **4**, 39–46.
17. J. Pan, C. Karlén and C. Ulfvin: 'Electrochemical study of resistance to localizad corrosion of stainless steel for biomedical applications', *J. Eletrochem. Soc.*, 2000, **147**, 1021–1025.
18. M. M. Beloti, J. M. D. A. Rollo, A. Itman Filho and A. L. Rosa: 'In vitro biocompatibility of dúplex stainless steel with and without 0.2% niobium', *J. Appl. Biomater. Biomech.*, 2004, **2**, 162–168.
19. K. Oh, Y. Kim, Y. Park and K. Kim: 'Properties of super stainless steels for orthodontic applications', *J. Biomed. Mater. Res. B*, 2004, **69B**, 183–194.
20. A. Kocijan and M. Conradi: 'The corrosion behaviour of austenitic and duplex stainless steels in artificial body fluids', *Mater. Technol.*, 2010, **44**, 21–24.
21. J. A. Platt, A. Guzman, A. Zuccari, D. W. Thornburg, B. F. Rhodes, Y. Oshida and B. K. Moore: 'Corrosion behavior of 2205 duplex stainless steel', *Am. J. Orthod. Dentofacial Orthop.*, 1997, **112**, 69–79.
22. 'Handbook of materials for medical devices', (ed. J. R. Davis), Chap. 3, 21–50; 2003, Materials Park, OH, ASM International.
23. J. B. Brunski: 'Biomaterials science – an introduction to materials in medicine', (ed. B. D. Ratner, et al.,). 2nd edn, 137–153; 2004, San Diego, CA, Elsevier Academic Press.
24. J. Douthett: 'Heat treating of stainless steels', in 'ASM handbook', (eds. S. R. Lampman and T. B. Zorc), 'Heat treating' **Vol. 4**. 9th edn, 1682–1757; 1991, Materials Park, OH, ASM International.
25. H. Okamoto and H. Baker: 'Metals handbook', 'Alloy phase diagrams' **Vol. 3**. 8th edn, 682; 1992, Materials Park, OH, ASM International.
26. D. M. E. Villanueva, F. C. P. Junior, R. L. Plaut and A. F. Padilla: 'Comparative study on sigma phase precipitation of three types of stainless steels: austenitic, superferritic and duplex', *Mater. Sci. Technol.*, 2006, **22**, (9), 1098–1104.
27. K. V. Sudhakar: 'Metallurgical investigation of a failure in 316L stainless steel orthopaedic implant', *Eng. Fail. Anal.*, 2005, **12**, 249–256.
28. O. E. M. Pohler: 'Failures of metallic orthopedic implants', in 'Metals handbook', (eds. W. T. Becker and R. J. Shipley), 'Failure analysis and prevention' **Vol. 11**, 2746–2749; 2002, Materials Park, OH, ASM International.
29. S. H. Teoh: 'Fatigue in biomaterials: a review', *Inter. J. Fatigue*, 2000, **22**, 825–837.
30. H. Sieurin: 'Fracture toughnessproperties of duplex stainless steels', 12–20; PhD thesis, Royal Institute of Technology, Stockholm, Sweden 2006
31. R. Johansson: 'Fatigue and fracture properties of duplex stainless steels', in 'ASM handbook', (ed. S. Lampman), 'Fatigue and fracture' **Vol. 19**, 757–768; 1996, Materials Park, OH, ASM International.
32. R. Ebara: 'Corrosion fatigue crack initiation behavior of stainless steels', *Proc. Eng.*, 2010, **2**, 1297–1306.
33. R. A. Perren, T. Suter, C. Solenthaler, G. Gullo, P. J. Uggowitzer, H. Böhni and M. O. Speidel: 'Corrosion resistance of super duplex stainless steels in chloride ion containing environments: investigations by means of a new microelectrochemical method. II: influence of precipitates', *Corros. Sci.*, 2001, **43**, 727–745.
34. Y. S. Ahn, J. M. Kim and B. H. Jeong: 'Effect of aging treatments and microstructural evolution on corrosion resistance of tungsten substituted 2205 duplex stainless steel', *Mater. Sci. Technol.*, 2002, **18**, (4), 383–388.
35. U. Kamachi Mudali, T. M. Sridhar and B. Raj: 'Corrosion of bio implants', *Sadhana*, 2003, **28**, 601–637.
36. Y. Ren, K. Yang, B. Zhang, Y. Wang and Y. Liang: 'Nickel-free stainless steel for medical applications', *J. Mater. Sci. Technol.*, 2004, **20**, 571–573.
37. M. Talha, C. K. Behera and O. P. Sinha: 'Promising in vitro performances of nickel-free nitrogen containing stainless steels for orthopaedic applications', *Bull. Mater. Sci.*, 2014, **37**, 1321–1330.
38. G. S. Frankel: 'Pitting corrosion', in 'Metals handbook', (ed. J. R. Davis), 'Corrosion fundamentals, testing and protection' **Vol. 13A**. 9th edn, 591–599; 2004, Materials Park, OH, ASM International.
39. R. A. Perren, T. A. Suter, P. J. Uggowitzer, L. Weber, R. Magdowski, H. Böhni and M. O. Speidel: 'Corrosion resistance of super duplex stainless steels in chloride ion containing environments: investigations by means of a new microelectrochemical method. I: precipitation-free states', *Corros. Sci.*, 2001, **43**, 707–726.
40. B. Deng, Y. Jiang, J. Gong, C. Zhong, J. Gao and J. Li: 'Critical pitting and repassivation temperatures for duplex stainless steel in chloride solutions', *Electrochem. Acta*, 2008, **53**, 5220–5225.
41. T. A. Palmer, J. W. Elmer and S. S. Babu: 'Observations of ferrite/austenite transformations in the heat affected zone of 2205 duplex stainless steel spot welds using time resolved X-ray diffraction', *Mater. Sci. Eng. A*, 2004, **A374**, 307–321.
42. M. Sawyer-Glover and F. G. Shellock: 'Pre-MRI procedure screening: recommendations and safety considerations for biomedical implants and devices', *J. Magn. Reson. Imaging*, 2000, **12**, 92–106.
43. H. Matsuura, T. Inoue, H. Konno, M. Sasaki, K. Ogasawara and A. Ogawa: 'Quantification of susceptibility artifacts produced on highfield magnetic resonance images by various biomaterials used for neurosurgical implants', *J. Neurosurg.*, 2002, **97**, 1472–1475.
44. P. Stradiotti, A. Curti, G. Castellazzi and A. Zerbi: 'Metal-related artifacts in instrumented spine. Techniques for reducing artifacts in CT and MRI: state of the art', *Eur Spine J.*, 2009, **18**, 102–108.
45. T. O. Woods: 'MRI safety and compatibility of implants and medical devices', in 'Stainless steels for medical and surgical applications', (eds. G. L. Winters and M. J. Nutt), 82–92; 2003, Pittsburgh, PA, ASTM International.